Journal of Neurophysiology

Encoding of Muscle Movement on Two Time Scales by a Sensory Neuron That Switches Between Spiking and Bursting Modes

J. T. BIRMINGHAM, Z. B. SZUTS, L. F. ABBOTT, AND EVE MARDER
Volen Center and Biology Department, Brandeis University, Waltham, Massachusetts 02454-9110

Birmingham, J. T., Z. B. Szuts, L. F. Abbott, and Eve Marder. Encoding of muscle movement on two time scales by a sensory neuron that switches between spiking and bursting modes. *J. Neurophysiol*. 82: 2786–2797, 1999. The gastropyloric receptor (GPR) neurons of the stomatogastric nervous system of the crab *Cancer borealis* are muscle stretch receptors that can fire in either a spiking or a bursting mode of operation. Our goal is to understand what features of muscle stretch are encoded by these two modes of activity. To this end, we characterized the responses of the GPR neurons in both states to sustained and rapidly varying imposed stretches. The firing rates of spiking GPR neurons in response to rapidly varying stretches were directly related to stretch amplitude. For persistent stretches, spiking-mode firing rates showed marked adaptation indicating a more complex relationship. Interspike intervals of action potentials fired by GPR neurons in the spiking mode were used to construct an accurate estimate of the time-dependent amplitude of stretches in the frequency range of the gastric mill rhythm (0.05–0.2 Hz). Spike trains arising from faster stretches (similar to those of the pyloric rhythm) were decoded using a linear filter to construct an estimate of stretch amplitude. GPR neurons firing in the bursting mode were relatively unaffected by rapidly varying stretches. However, the burst rate was related to the amplitude of long, sustained stretches, and very slowly varying stretches could be reconstructed from burst intervals. In conclusion, the existence of spiking and bursting modes allows a single neuron to encode both rapidly and slowly varying stimuli and thus to report cycle-by-cycle muscle movements as well as average levels of muscle tension.

INTRODUCTION

Sensory neurons use a variety of coding strategies to deal with the wide dynamic range of the stimuli to which they respond. Some sensory neurons respond phasically to a signal, that is, their firing rates are initially affected by rapid changes in the stimulus but subsequently adapt. Other sensory neurons show considerably less or no adaptation and encode sustained stimulus intensities. An advantage of sensory neurons that show adaptation is that they can report changes in stimulus intensity over a very large range, whereas neurons that do not have appreciable adaptation may only be able to report stimulus intensity over a more limited range of values. It is often assumed that information about changes in stimulus intensity and information about sustained stimuli are encoded by different neurons. In this paper we demonstrate that a single muscle stretch receptor neuron can encode information over two different time scales by firing in two modes, spiking and bursting. Information about rapid changes in muscle stretch is encoded by interspike intervals, whereas information about sustained muscle length is encoded by burst intervals.

The gastropyloric receptor (GPR) neurons are two bilateral pairs of stretch-sensitive neurons that provide sensory input to the stomatogastric nervous system of the crab *Cancer borealis* (Katz et al. 1989). The stomatogastric nervous system of *C. borealis* is a small, well-studied neural network that controls stomach movements (Harris-Warrick et al. 1992). The 25–26 motor neurons (Kilman and Marder 1996) in the *C. borealis* stomatogastric ganglion (STG) can be divided roughly into two groups: those innervating the muscles that move three teeth in the gastric mill (chewing) and those innervating the muscles that dilate and constrict valves in the pylorus (filtering) (Maynard and Dando 1974). The pyloric rhythm has a period of 0.5–2 s (Harris-Warrick et al. 1992), whereas the period of the gastric mill rhythm is typically 5–20 s (Coleman et al. 1995; Mulloney and Selverston 1974a,b). Gastropyloric receptor neuron 2 (GPR2) innervates both a gastric mill muscle *gm9* and a pyloric muscle *cpv3a*. Katz et al. (1989) found that GPR2 fired action potentials in response to either passive stretch or nerve-evoked contraction of the innervated muscles. In response to two second duration ramp-and-hold stretches, the GPR2 firing rate showed modest adaptation, and the number of spikes varied linearly with either the muscle length or tension (Katz et al. 1989). In some preparations, GPR2 was observed to fire rhythmic bursts of action potentials in the absence of any apparent sensory stimulus (Katz et al. 1989). In this paper, we study quantitatively the encoding properties of GPR2 in the two modes that Katz et al. (1989) initially described.

METHODS

Animals and solutions

Adult crabs, *Cancer borealis* were obtained from local seafood suppliers and kept stored in aerated aquaria at 12–15°C. We used physiological saline with the following composition (in mM): 440 NaCl, 11.3 KCl, 13.3 $CaCl_2$, 26.3 $MgCl_2$, 5.2 maleic acid, and 11.0 Trizma base, pH 7.4–7.5.

Physiology

The STG and muscles were dissected according to Hooper et al. (1986). The stomach was removed from the animal, slit ventrally from the esophagus to the midgut, and pinned flat in a dissecting dish. The anterior ganglia, STG, and nerves and muscles associated with the GPR2 neuron from one side of the animal were removed and pinned in 20-ml silicone elastomer (Sylgard)–coated (Dow Corning, Midland, MI) Petri dishes. After confirming the presence of a pyloric rhythm, we cut the dorsal ventricular nerve (*dvn*), isolating the GPR2 neuron and muscles from the STG (Fig. 1). During recording sessions,

The costs of publication of this article were defrayed in part by the payment of page charges. The article must therefore be hereby marked "*advertisement*" in accordance with 18 U.S.C. Section 1734 solely to indicate this fact.

0022-3077/99 $5.00 Copyright © 1999 The American Physiological Society

Downloaded from jn.physiology.org on November 10, 2005

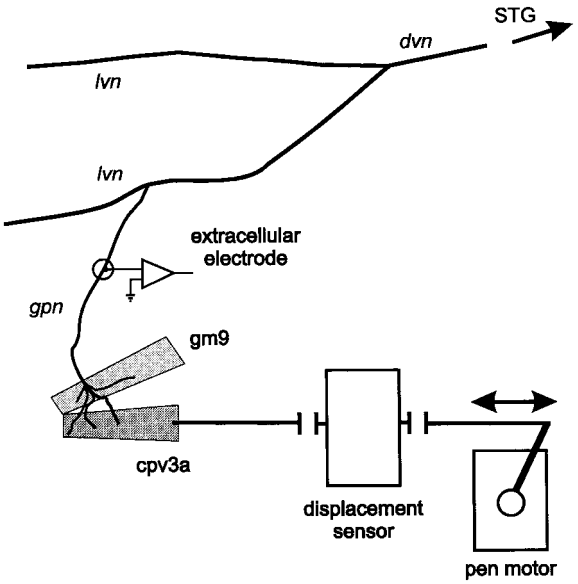

FIG. 1. Schematic of experimental setup. The dissection consists of the gastropyloric nerve (*gpn*), the lateral ventricular nerve (*lvn*), the dorsal ventricular nerve (*dvn*), and the *gm9* and *cpv3a* muscles. The origin of *cpv3a* is pinned to the dish. The insertion is attached to the arm of a pen motor via a Grass displacement sensor using a silk thread. Extracellular activity in the *gpn* is monitored using a stainless steel pin or suction electrode.

the preparations were continuously superfused (~10 ml/min) with saline cooled to 11–13°C. Extracellular measurements of the activity in the gastropyloric nerve (*gpn*), which contains the GPR2 axon, were made using stainless steel bipolar pin electrodes or glass suction electrodes, amplified by an AM-Systems 1700 differential amplifier (Carlsborg, WA), and recorded using an Axon Instruments (Foster City, CA) data interface board. Spike times were extracted from extracellular recordings using the program Datamaster developed in our laboratory by W. Miller and C. Howe and were analyzed using routines written in Matlab (The MathWorks, Natick, MA). All of the motor axons that project into the *dvn* bifurcate and then project into both lateral ventricular nerves (*lvns*), whereas the GPR axons project up only in the ipsilateral *lvn*. To be certain that action potentials measured in the *gpn* were from GPR2 and not a motor axon, we often placed another extracellular electrode on the contralateral *lvn* and confirmed that the action potentials were not observed.

Muscle stretching

For all measurements, we stretched the *cpv3a* muscle (Maynard and Dando 1974). The muscle origin was pinned to the Sylgard-coated dish (Fig. 1). The insertion was attached to a Grass force-displacement transducer (Model FT03, Quincy, MA) via no. 6 suture thread. The transducer in turn was attached to the lever arm of a chart recorder pen motor [removed from a defunct Gould 440 (Cleveland, OH)] via another thread. Because the thread between the muscle insertion and the transducer was taut and much less elastic than the muscle, in this configuration the transducer measures muscle length (Fig. 1). The pen motor was driven and hence the muscle stretched using voltage waveforms generated on a Pentium 266 MHz computer using the data acquisition program LabView (National Instruments). In the decoding experiments we stretched the muscle with filtered white noise. The white noise was generated using the computer and was filtered by passing it through a single pole RC filter. The muscle displacement was measured using the displacement transducer and calibrated visually to ±0.02 mm using an eyepiece with a reticule. Before each experiment the transducer was adjusted so that the muscle was completely extended (relaxed length 2–3 mm) but under no tension. The muscle was then stretched (<0.1 mm) until a threshold response was observed and then slightly relaxed.

Decoding techniques

GPR2 fires either in a spiking or bursting mode. We used two techniques, interspike interval (ISI) decoding and linear filters, to generate an estimate $S_{est}(t)$ of the muscle stretch waveform $S(t)$ that evoked a given spike train with spike times t_i, $i = 1, 2, \ldots$ in a GPR2 preparation in the spiking mode. We found that we could use an interspike interval code to describe the encoding of stretch when the stimulus varied slowly compared with the interspike interval. The interspike interval at spike time t_i is the time since the last spike, $t_i - t_{i-1}$. Because increased stretch amplitude results in decreased interspike interval, it is useful to define a "rate" at each spike time by inverting the interspike interval, $R(t_i) = (t_i - t_{i-1})^{-1}$. When stretch increases, this rate increases. To construct an ISI decoding relationship, we stretched the muscle with waveform $S(t)$ and calculated $R(t_i)$ for all values of i. We then plotted $S(t_i)$ versus $R(t_i)$ for each of the spike times and fit a function $\bar{S}(R)$ to the data points using the SigmaPlot program (Jandel Scientific, San Rafael, CA.) The function was of the form $\bar{S}(R) = A + B(1 - e^{-CR})$, where A, B, and C are free parameters used in the fit. For small values of R, $\bar{S}(R)$ depends linearly on R. For large values of R, $\bar{S}(R)$ approaches a constant. To decode another spike train with spike times t_j, $j = 1, 2, \ldots$ we computed $R(t_j)$ and constructed an estimate of the stretch S_{est} at time t_j as $\bar{S}[R(t_j)]$. Between spike times, $R(t)$ was defined by linear interpolation.

We used the technique of linear filters (Rieke et al. 1997) to reconstruct the stretch stimulus from spike times for spiking GPR2 neurons when the stimulus varied rapidly. From spike times t_i, $i = 1, 2, \ldots N$, we constructed an estimate of the stimulus $S_{est}(t)$ using a linear kernel $K(t)$ and a constant S_0

$$S_{est}(t) = S_0 + \sum_{i=1}^{N} K(t - t_i) \quad (1)$$

S_0 is the threshold stretch required for spike generation. $K(t)$ describes the stimulus at times just preceding and following a stretch. The linear summation of the kernels for each spike is equivalent to the assumption that each spike contributes independently to the estimation of the stimulus. S_0 and $K(t)$ were determined by minimizing the error E between the estimate and actual stimulus during some training interval $0 < t < T$, where

$$E^2 = \int_0^T |S(t) - S_{est}(t)|^2 dt \quad (2)$$

To reduce the computation time, we only defined $S(t)$ at 50-ms intervals and rounded the spike times t_i to the nearest integral multiple of 50 ms. We did not constrain the kernel $K(t)$ to be causal but assumed that it was nonzero only in the 2 s preceding and the 2 s after a spike. For each of a range of values of S_0 between the minimum and maximum value of the stimulus, we determined the best $K(t)$ using a stochastic gradient descent algorithm (Abbott 1994). We estimated the stretch waveform that generated a novel spike train (not included in the training interval) from *Eq. 1*, using the optimum S_0 and $K(t)$ pair.

When the GPR2 neuron was in the bursting mode, we used a burst interval (BI) decoding scheme to interpret the burst train and to estimate the stretch. The burst interval, BI, is the time from the start of the previous burst to the start of the present burst. The decoding procedure was identical to that used with spiking mode neurons, except in this case t_i referred to the start time of the ith burst. The duration of the burst was not used in the decoding.

For each of our estimates of the stimulus $S_{est}(t)$, $0 < t < T$, constructed using the ISI decoding method, the BI decoding method,

Journal of Neurophysiology

Downloaded from jn.physiology.org on November 10, 2005

or the linear filter technique, we calculated a normalized root-mean-square (RMS) error E_{norm}

$$E^2_{norm} = \frac{\int_0^T |S(t) - S_{est}(t)|^2 dt}{\int_0^T |S(t) - S_{mean}|^2 dt} \quad (3)$$

where S_{mean} is the mean of the true stretch $S(t)$ over the test interval. Estimating the $S(t)$ by S_{mean} results in a value of 1 for E_{norm}. Values of E_{norm} near 0.7 result from reconstructions that appear excellent by eye.

RESULTS

GPR2 neurons show two modes of activity, spiking and bursting

Figure 2*A* shows the response of a GPR2 neuron to a rapid muscle stretch. The GPR2 response began soon after the start of the stretch. During the first few hundred milliseconds of firing, the instantaneous firing rate (the reciprocal of the interspike interval) adapted rapidly, falling from >20 Hz to ~5 Hz. The rate continued to decrease during the next 6 s before stabilizing near 2.5 Hz. The cell stopped firing when the muscle was released. We define GPR2 neurons with this kind of behavior as being in the *spiking mode*. In the absence of a stretch stimulus, spiking mode neurons were either quiescent or fired at a slow (<1 Hz) rate. Thirty-seven of 58 GPR2 neurons were in the spiking mode at the start of our recordings.

Figure 2*B* illustrates the behavior of GPR2 neurons that we define as being in the *bursting mode*. During the 4 min preceding the stimulus, the neuron shown in Fig. 2*B* fired bursts of action potentials with a burst period of 63.1 ± 2.8 (SD) s. We then gave a train of 3-s duration stretches at 30-s intervals. This entrained the bursting to a 30-s period. During the 3 min after the periodic muscle stretch was stopped, the burst period was 65.7 ± 2.1 s. Twenty-one of 58 GPR2 neurons were in the bursting mode at the start of our recordings. The average burst period of unstretched bursting mode preparations ranged from 12 to 101 s. The mean average burst period was 32.7 ± 20.1 s (n = 21) in the absence of stretch.

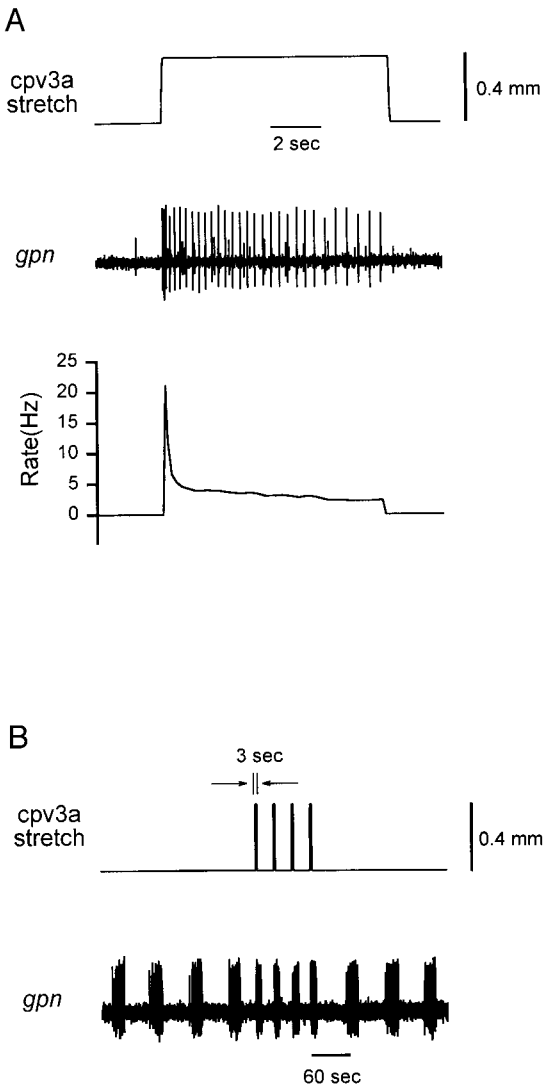

FIG. 2. *A*: gastropyloric receptor neuron 2 (GPR2) in spiking mode responding to a rapid *cpv3a* muscle stretch. *Top trace*: imposed stretch measured by the transducer. *Middle trace*: extracellular recording of GPR2 action potentials on the *gpn*. *Bottom trace*: instantaneous firing rate calculated from interspike intervals. *B*: GPR2 neuron in bursting mode responding to rapid *cpv3a* muscle stretches. *Top trace*: a series of 3-s duration, 30-s period stretches. *Bottom trace*: extracellular recording of GPR2 action potentials on the *gpn*.

Response of spiking mode GPR2 neurons to persistent (DC) and time-varying (AC) stretches

We wished to characterize the response of spiking GPR2 neurons to stimuli that varied in amplitude, rise-time, and duration. We used long duration constant stretches to characterize the persistent response (we call this the DC stimulus), and we employed sine waves to characterize the phasic response (we call this the AC stimulus). We chose 3 s as the period of the time-varying stimulus because this is between the periods of the pyloric and gastric mill rhythms.

Figure 3*A* shows the response of a spiking mode GPR2 neuron when unstretched and in response to persistent stretches of 0.23 and 0.51 mm. Each recording was made after allowing the firing rate to stabilize (~5 s). Figure 3*B* shows the equilibrium firing rate in response to DC stretches for five spiking preparations. Here, "equilibrium rate" means the average rate after spike rate adaptation has taken place. To calculate the equilibrium firing rate for a given stretch amplitude, we stretched the muscle, waited 15 s, and then counted the number of spikes fired during the next minute. We then released the stretch and waited 2 min before making the next measurement. For each preparation, the equilibrium firing rate increased with amplitude for stretches up to 0.5 mm. Linear fits to the data sets showed that the sensitivity to stretch measured in Hz/mm varied over a factor of three for the five preparations. Analysis of variance (ANOVA, 1-way) of the entire data set showed a statistically significant ($P < 0.001$) dependence of the firing rate on amplitude. We note that the maximum equilibrium firing rate observed at any amplitude was ~4.5 Hz.

Figure 4*A* shows the response of a spiking mode GPR2 neuron to a series of sine wave (3-s period) stretches with the same mean (DC component) value but different AC amplitudes. The amplitude of the DC component of the

Journal of Neurophysiology

Downloaded from jn.physiology.org on November 10, 2005

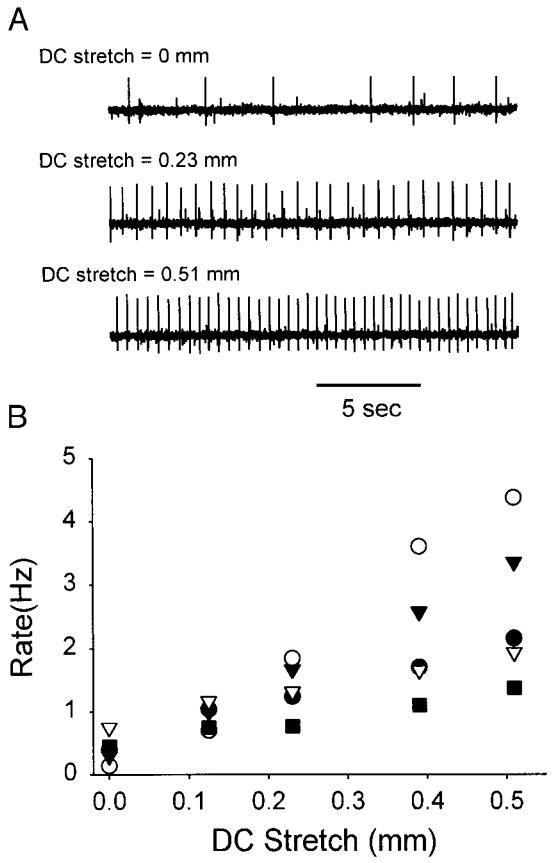

FIG. 3. Spiking mode GPR2 response to DC stretch. *A*: extracellular measurements of GPR2 responses in the absence of stretch and during stretches of 0.23 and 0.51 mm. *B*: summary of experiments on 5 preparations. In each experiment (shown as a different symbol), the muscle was stretched and held at the amplitudes shown. After waiting 15 s for the firing rate to equilibrate, we calculated the persistent firing rate by counting the spikes fired during the next minute.

stretch was 0.3 mm, which prevented the muscle from becoming completely relaxed during the minima of the stretch. As the amplitude increased, the number of spikes fired during each period increased, and the spikes became more tightly clustered, firing at a nearly constant phase with respect to the stimulus.

To describe the relationship between AC stretch amplitude and GPR2 activity, we computed the instantaneous firing rate for the experiment shown in Fig. 4*A*. The dependence of the average instantaneous firing rate on the AC amplitude is plotted in Fig. 4*B*. The average instantaneous firing rate was that calculated from all interspike intervals over a 60-s time period. As the AC amplitude increased, the rate increased dramatically. The average instantaneous firing rates from six preparations and two AC amplitudes are shown in Fig. 4*C*. The increase in the rate with increased amplitude was highly significant ($P < 0.003$).

Response of bursting mode GPR2 neurons to persistent (DC) and time-varying (AC) stretches

Figure 2*B* shows that GPR2 neurons in the bursting mode responded to muscle stretch. We repeated the DC and AC stretch experiments that had been done on spiking mode neurons to determine whether a different aspect of stretch is encoded in the bursting mode. Figure 5*A* shows the response of a GPR2 neuron to sustained stretch. The response before any stretch was applied is shown in the *top trace*. The average burst period was 79.3 ± 14.2 s. The *second trace* shows the response during a 0.2-mm DC stretch, 5 min in duration. The average burst period was 39.1 ± 1.8 s. The *third trace* shows the response during a 0.35-mm stretch. The average burst period

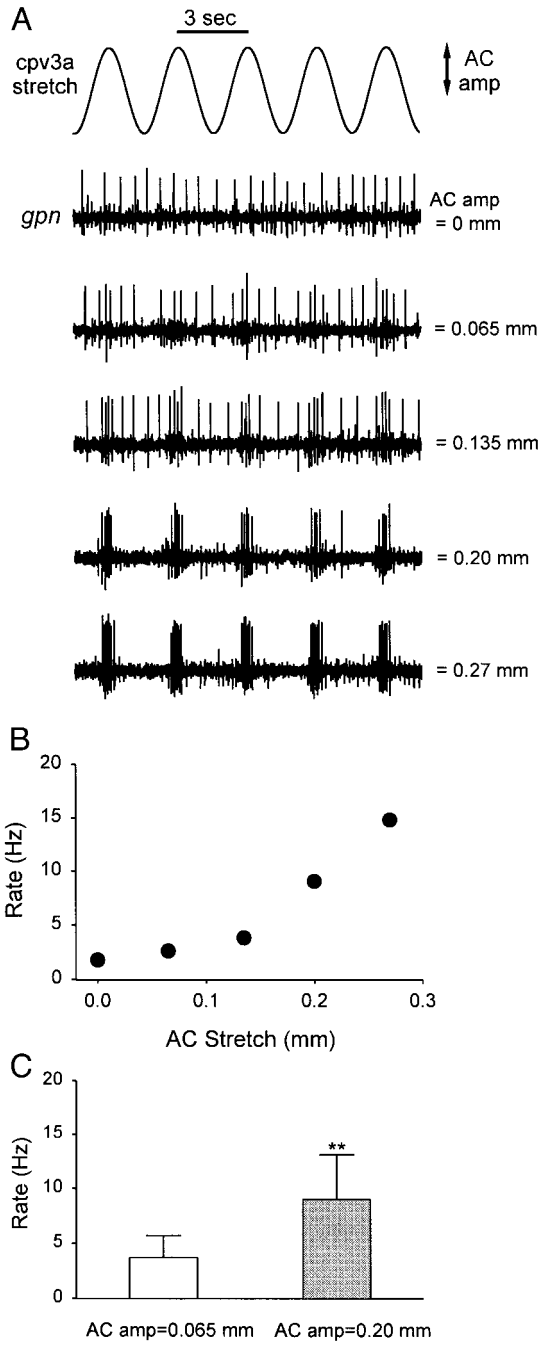

FIG. 4. Spiking mode GPR2 neuron response to AC stretch. *A*: imposed 3-s period sinusoidal stretches with AC amplitudes 0.0, 0.065, 0.135, 0.20, and 0.27 mm and corresponding extracellular measurements of GPR2 response. *B*: plot of average instantaneous firing rate as a function of *cpv3a* AC stretch amplitude for the spiking mode GPR2 preparation shown in *A*. Each rate was calculated from 1 min of stretch. *C*: average firing rate for 6 spiking preparations during 1-min AC stretches of 0.065 and 0.20 mm. The increase was significant (Student's *t*-test, $P < 0.003$.)

Journal of Neurophysiology

Downloaded from jn.physiology.org on November 10, 2005

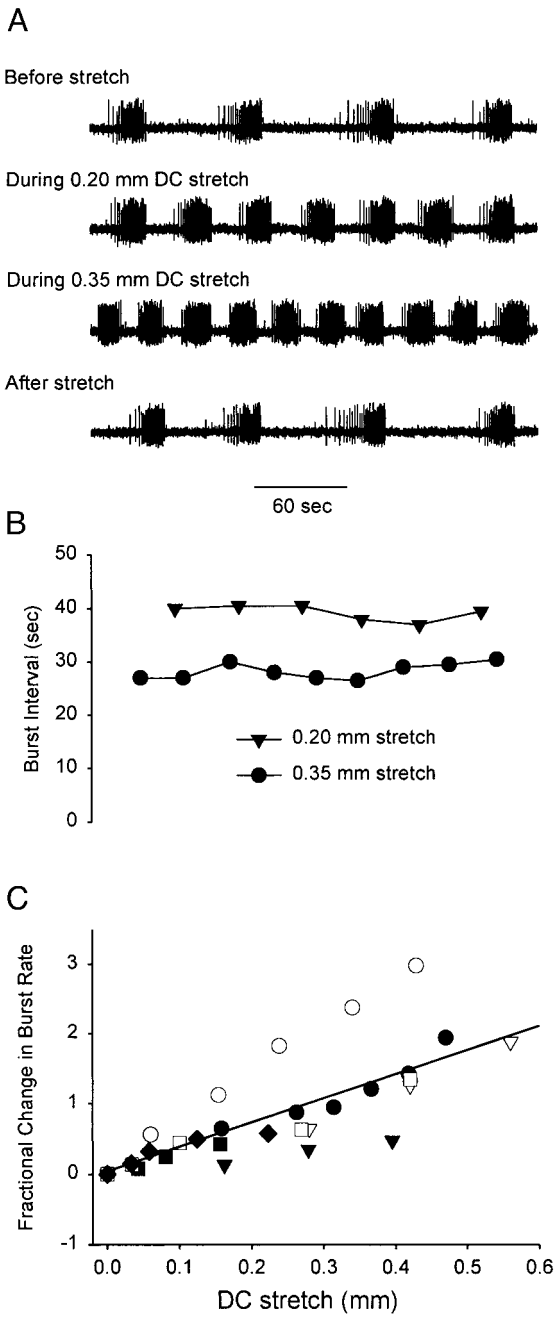

FIG. 5. Bursting mode response to DC stretch. *A*, *top trace*: extracellular recording of GPR2 activity in an unstretched preparation. *Second trace*: extracellular recording during 0.20-mm DC stretch. *Third trace*: extracellular recording during 0.35-mm DC stretch. *Bottom trace*: extracellular recording 2 min after release from 0.35-mm DC stretch. *B*: plot of burst intervals for 0.20- and 0.35-mm stretches during the time shown in *A*. The time bar for *A* also pertains for the plot in *B*. *C*: plot of the increase in bursting rate at different DC amplitudes compared with the bursting rate when the preparation was unstretched. The data are pooled from 7 bursting mode experiments, each shown as a different symbol. The solid line is the best linear fit to the data (see text).

was 29.0 ± 2.2 s. After the release of the muscle from the larger stretch, the bursting stopped for 2 min (missing 1 burst) and then resumed (*bottom trace*). The average period during the next 5 min was 74.5 ± 13.0 s. Figure 5*B* is a plot of the burst interval for the two stretches during the time shown in Fig. 5*A*. It remained relatively constant and did not adapt during the two imposed stretches.

Because the burst period decreases with increased DC stretch, it is useful to define the equilibrium bursting "rate" to be the inverse of the average burst period. We determined the relationship between the equilibrium bursting rate and the amplitude of DC stretch for seven preparations stretched to a range of DC amplitudes. For each measurement we stretched the muscle from the rest length, held it at a particular length for 5 min, and measured the average burst period. Between stretches we waited 5 min. The average burst period of unstretched preparations varied between 20 and 101 s. For purposes of comparison, we normalized the burst rates of each preparation to the rates when the preparations were unstretched, and we computed the fractional changes in the burst rate. These are plotted in Fig. 5*C*, where each symbol corresponds to a different preparation. In all cases the burst rate increased with stretch with an approximately linear dependence. The solid line is the best linear fit to the pooled data and has a *Y* intercept of 0.04 and a slope of 3.47/mm. There was a significant association between the bursting rate and stretch (1-way ANOVA, $P < 0.001$, $F = 70.4$).

Figure 6*A* shows the response of a bursting preparation to sinusoidal stretches (3-s period) with amplitude ranging from 0 to 0.27 mm. When the AC amplitude was increased from 0 to 0.135 mm the average burst period remained almost constant (29.0 vs. 29.7 s), although the timing of the burst onsets was affected. With increased amplitude, the bursts became more likely to be triggered by stretch, and hence individual burst periods tended toward multiples of the 3-s stimulus period. Increasing the AC amplitude to 0.20 mm decreased the average period to 25.6 s. When a 0.27-mm AC stretch was used, the average period decreased slightly to 24.4 s. In between bursts, spikes phase-locked to the stimulus were fired, as shown in the *inset*. In this case, GPR2 reports information about the fast component of the stimulus in the phase-locked spikes and information about the slow component, that is the DC stretch, in the average burst frequency. It is interesting to note that the bursting mode GPR2 response to the sinusoidal stretch during the interburst interval (Fig. 6*A*, *inset*) is much smaller that when it is in the spiking mode (Fig. 4*A*).

Figure 6*B* shows the dependence of normalized burst rate on AC amplitude for five bursting preparations. Again, the rate was normalized to the unstretched rate to facilitate comparison. Each data point was measured from 5 min of stretch. The solid line is the best linear fit to the data and has a *Y* intercept of 0.01 and a slope of 0.065/mm. There was no significant association between the bursting rate and stretch (1-way ANOVA, $P = 0.695$, $F = 0.157$).

GPR2 can switch between the spiking mode and the bursting mode

During stretch experiments, 14 of the 37 preparations originally in the spiking mode switched into the bursting mode. In three cases we observed this to occur suddenly while the *cpv3a* muscle was being stretched. Figure 7 shows one of these transitions. While the neuron was in the spiking mode, the firing rate increased sharply with incremental stretches of the *cpv3a* muscle, each time adapting to an equilibrium value after a few seconds, as shown in the *left inset*. As the stretch was

Journal of Neurophysiology

Downloaded from jn.physiology.org on November 10, 2005

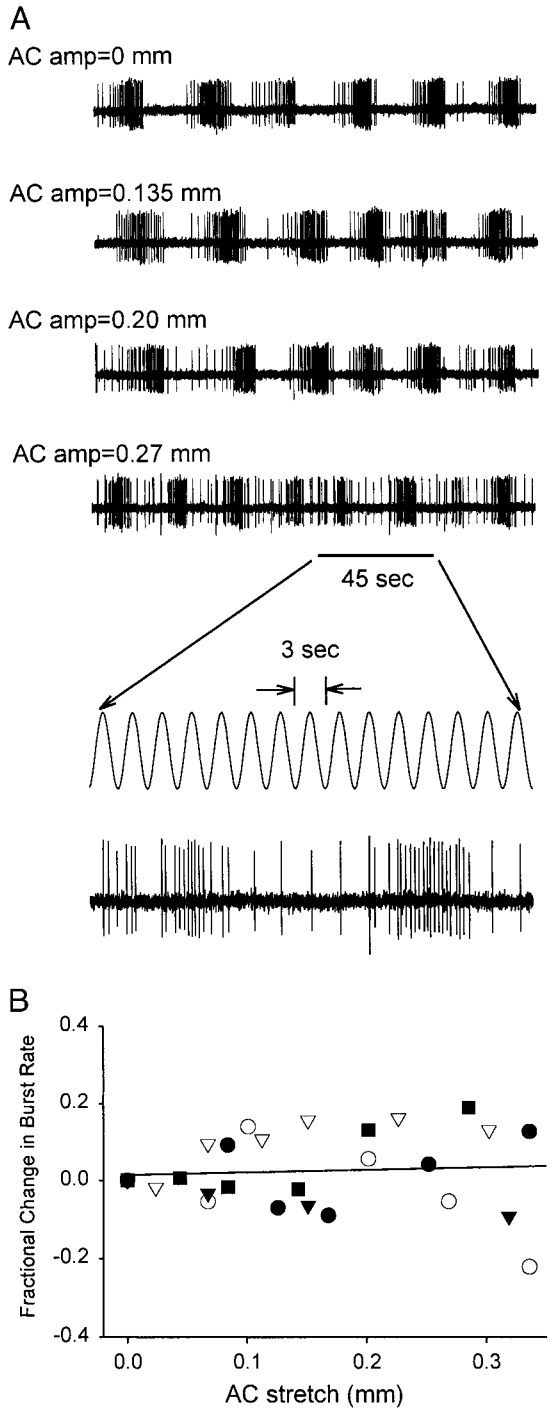

FIG. 6. Bursting mode response to AC stretch. *A, top trace*: extracellular recording of GPR2 activity in an unstretched preparation. *Second trace*: extracellular recording during 0.135-mm AC (3-s period) stretch. *Third trace*: extracellular recording during 0.20-mm AC stretch. *Bottom trace*: extracellular recording during 0.27-mm AC stretch. *Inset*: expanded view of *bottom trace* showing response to 0.27-mm AC stretch of *cpv3a*. *B*: plot of the increase in bursting rate at different AC amplitudes compared with the bursting rate when the preparation was unstretched. The data are pooled from 5 bursting mode preparations, each shown as a different symbol. Solid line is the best linear fit to the data (see text).

increased beyond 0.3 mm, the equilibrium firing rate became less sensitive to changes in stretch. When the rate was ~4.5 Hz, the cell spontaneously switched into the bursting mode while the stretch was being held constant, as shown in the *right inset*. Further stretch while in the bursting mode resulted in an increased burst rate. When the muscle was allowed to relax, GPR2 switched back to the spiking mode. An immediate repetition of a large stretch did not result in a return to the bursting mode, and hence the transition into the bursting mode is not triggered simply by stretching the muscle past a threshold length. The sudden transitions into the bursting mode always occurred during a stretch >0.35 mm. However, in two other preparations we were unable to induce the switch from spiking to bursting even when applying a 0.5-mm DC stretch for 30 min.

Conversely, we observed a preparation initially in the bursting mode switch into the spiking mode. Figure 8 shows five 3-min snapshots taken during 16 h of GPR2 activity in a preparation initially in the bursting mode in the absence of muscle stretch. There was no stretch imposed at any time during the 16 h. The initial burst period was very short, 13 s. One hour later, the preparation was not bursting at all, but rather firing spikes at a rate of 1 Hz. In the traces 6, 11, and 16 h after the first measurement, we see that the neuron returned to the bursting mode. During the experiment, the average burst period, as well as the burst duration and intraburst firing frequency, varied considerably.

Very slowly varying stretches can be decoded from bursts using a burst interval code

Can the timing of bursts or spikes be used to reconstruct the muscle stretch waveform that generated them? Two observations from the experiments described above suggested that a simple decoding scheme could be used to reconstruct slowly varying stretch waveforms from burst intervals. First, the average burst frequency depended sensitively on stretch amplitude. Second, there was no adaptation of the bursting rate (Fig. 5*B*), indicating that the bursting rate depended primarily on stretch amplitude but not on its derivative (velocity) or integral (history).

To test the BI decoding hypothesis, we stretched a *cpv3a* muscle for 30 min with a slowly varying random waveform. The waveform consisted of computer-generated white noise filtered using an RC low-pass filter with a 1,000-s time constant. The first 15 min of the stretch were used to determine the relationship between stretch and burst interval. As discussed in METHODS, it is convenient to define a burst rate $R(t_i) = (t_i - t_{i-1})^{-1}$ for each of the bursts. We measured the start times t_i of the bursts, and in Fig. 9*A* we plot the stretch $S(t_i)$ versus the $R(t_i)$ as solid circles. The solid line is a fit to the data $\bar{S}(R) = [-0.76 + 1.16(1 - e^{-56.7R})]$mm, where R is measured in hertz. At low burst rates, the relationship is close to linear, consistent with the results from Fig. 5*C*. For the largest stretches, we observed a flattening of the stretch versus rate curve, indicating that, for the larger amplitudes, more variability in the burst rate was observed. This variability may arise from a secondary dependence of the rate on stretch velocity or another higher order characteristics of the stretch. We tested the BI decoding scheme using the second 15 min of the data set. We measured the burst start times and again computed $R(t_i)$. Between bursts, we linearly interpolated to obtain $R(t)$ for all times. We predicted the stretch waveform at each time t

Journal of Neurophysiology

Downloaded from jn.physiology.org on November 10, 2005

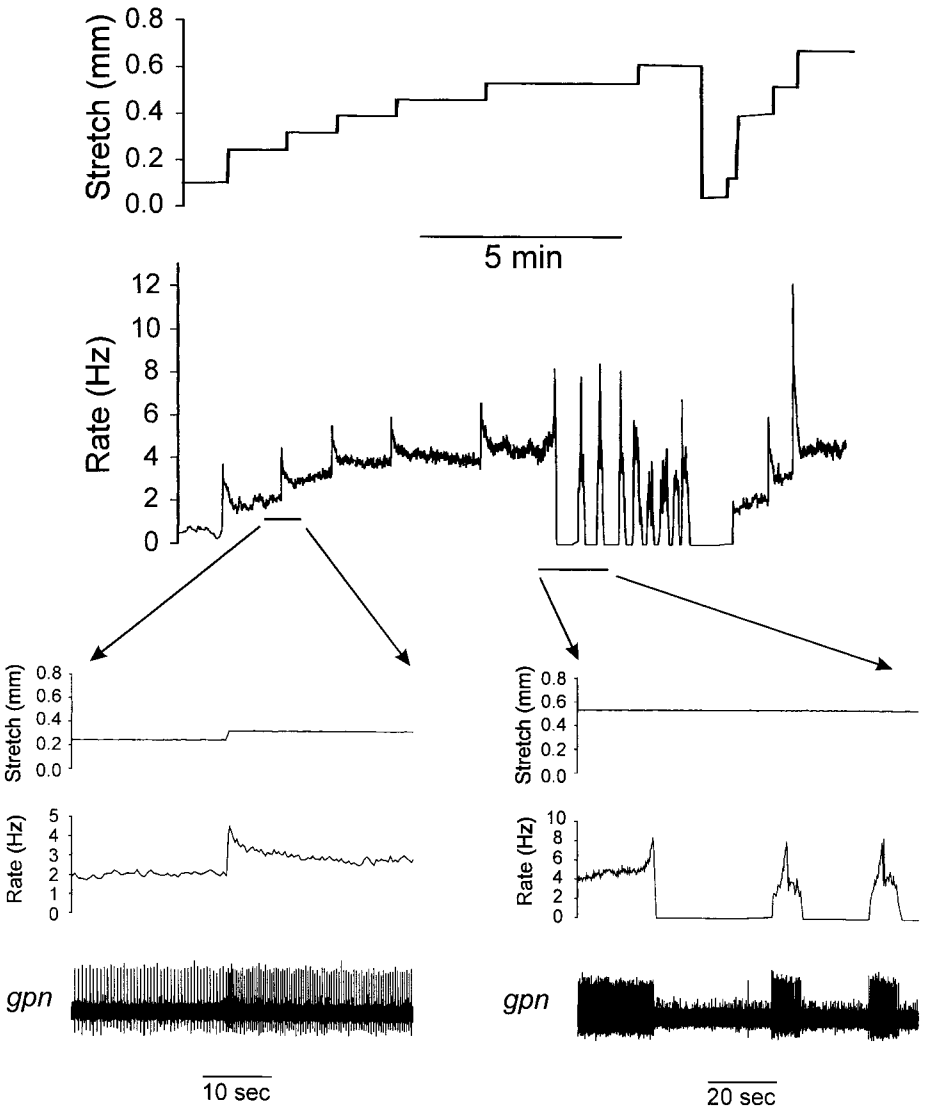

FIG. 7. GPR2 neuron initially in the spiking mode can switch to the bursting mode during *cpv3a* muscle stretch. *Top panel*: stretch imposed on a *cpv3a* muscle in a preparation initially in the spiking mode. *Middle panel*: instantaneous firing rate of GPR2 calculated from the inverse of the interspike interval. *Left* and *right insets* below show expanded views of the firing rate and the response measured extracellularly while the neuron was in the spiking and bursting modes, respectively.

to be $\bar{S}[R(t)]$. Figure 9*B* shows the actual waveform (black) and the prediction (red). The E_{norm} (*Eq. 3*) between this prediction and the actual stretch was 0.76.

As the filter time constant is reduced, we expect that the ability of the BI decoding scheme to reconstruct the stimulus will decrease. Eventually, when the characteristic time of the stretch waveform is comparable to or smaller than the average burst interval, BI decoding will not work because the burst interval will report only the mean stretch amplitude. We varied the time constant τ used to filter the white noise and found that the decoding scheme could still be used when τ was reduced to 100 s, but that it could not be used when τ was reduced to 10 s or smaller. Figure 9*C* shows the response of a bursting mode GPR2 neuron to a white noise stimulus filtered with τ = 10 s (black trace). The dashed lines mark the start times of the bursts. The red trace shows the calculated burst rate. Although the burst interval is no longer useful for BI decoding, bursts still provide some information about a fast stimulus, because the bursts tend to be triggered by large positive slopes or peaks in the stretch waveform. When the waveform is very fast (τ = 0.1 s), even those features are ignored by the bursting mode.

Slowly varying (gastric mill-like) stretch waveforms can be decoded from spikes using an interspike interval code

Can the interspike interval similarly be used to reconstruct the stimulus from spike times when GPR2 is in the spiking mode? The spiking mode is a less likely candidate for this than the bursting mode because of adaptation; the firing rate is a function not only of the stretch amplitude, but also of the recent stretch history (Fig. 2). We stretched spiking mode GPR2 preparations with white noise waveforms filtered over a range of time constants to determine whether and when an ISI decoding scheme would work. In Fig. 10*A* we show a portion of an experiment where a spiking mode preparation was stretched with a slow (τ = 1,000 s) waveform (black trace). The resulting instantaneous GPR2 firing rate is plotted in red. When the amplitude was large for a long period of time, the firing rate adapted considerably. Figure 10*B* plots the relationship between stretch and rate for three 40-s intervals *S1–S3* of the waveform shown in Fig. 10*A*. Although the stretch extended over different ranges of amplitudes during the three intervals, the instantaneous firing rate varied over overlapping intervals.

Journal of Neurophysiology

Downloaded from jn.physiology.org on November 10, 2005

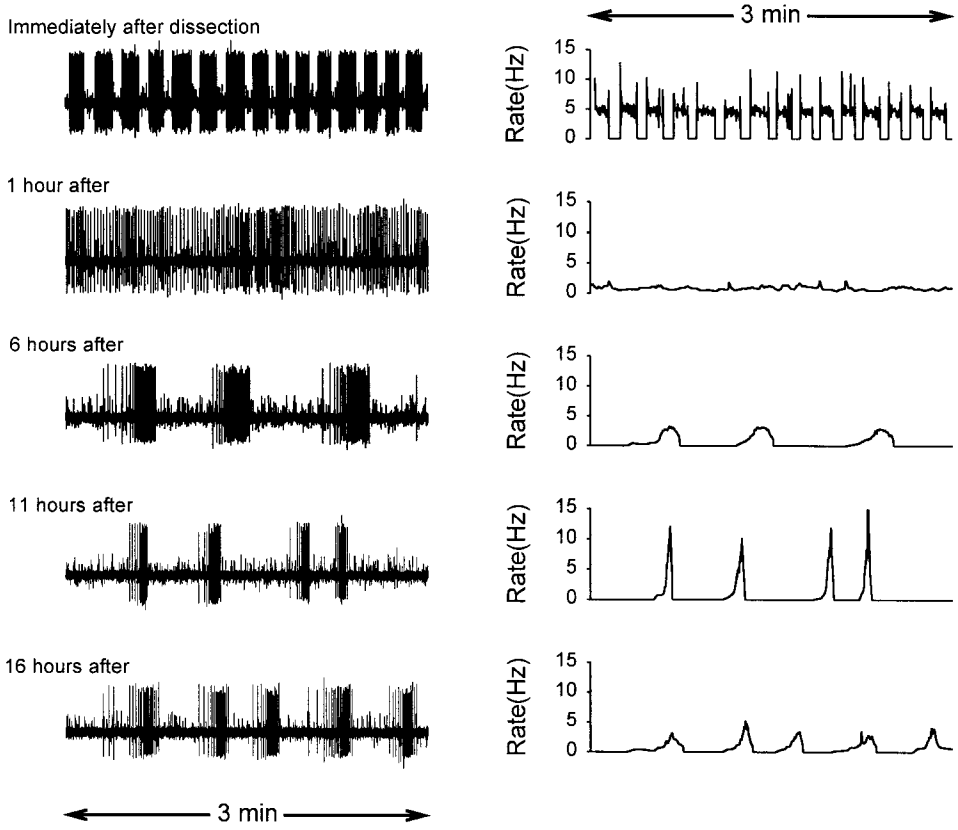

FIG. 8. GPR2 neuron initially in the bursting mode can show a range of spontaneous activities. *Left panels* (*top* to *bottom*): extracellular recordings of spontaneous GPR2 activity immediately after dissection, and 1, 6, 11, and 16 h later. *Right panels*: corresponding instantaneous firing rates for each of the recordings.

Hence a unique stretch-rate relationship could not be defined, and accurate ISI decoding was not possible.

We found that the history dependence of the firing rate seen in Fig. 10, *A* and *B*, was not a problem when the waveform varied over a fast enough time scale ($\tau = 10$ s). We stretched the same preparation for 10 min with white noise filtered with $\tau = 10$ s. Figure 10*C* shows the relationship between stretch and firing rate during the first 5 min of the stretch. The solid circles are data points. The curve is a fit to the data: $\bar{S}(R) = 0.432(1 - e^{-1.239R})$ mm, where R is measured in hertz. No systematic variation in the stretch-rate relationship was observed when different subintervals of the data set were examined. ISI decoding was used to reconstruct the waveform from the spike times during the second 5 min of the experiment. A portion of the reconstruction is shown in Fig. 10*D*. The actual waveform is shown in black and the ISI decoding prediction is in red. E_{norm} for the reconstruction of the entire 5 min was 0.67. The typical period of the gastric mill rhythm is 10–20 s, and hence the interspike interval might be useful for decoding spikes generated by muscle movements generated during this motor pattern.

A linear filter successfully decodes spikes for pyloric frequency stretches

When the characteristic time of the stretch waveform is comparable to or smaller than the average interspike interval, ISI decoding cannot capture the details of the stretches between the action potentials. The GPR2 neuron, as we have seen, fires at average rates of a few hertz in response to *cpv3a* stretch, and, as expected, we found that the decoding method performed poorly when τ was reduced below 1 s. Using a spiking mode GPR2 preparation, we stretched the *cpv3a* muscle for 3 min using filtered white noise with $\tau = 0.3$ s. We used the first 90 s of the stretch to determine the relationship between stretch and instantaneous spiking rate shown in Fig. 11*A*. The data are the solid circles, and the curve is a fit to the data: $\bar{S}(R) = [0.187 + 0.217(1 - e^{-0.280R})]$ mm, where R is measured in hertz. The data and fit reflect two observations. *1*) For firing rates below 4 Hz, the clustering of points is almost vertical. A firing rate of 1.5 Hz could result from a stretch amplitude anywhere between 0.15 and 0.3 mm with almost equal probability. The fit chooses some average stretch. *2*) The curve is almost completely flat for rates above 4 Hz. We tested the ISI decoding method on the second 90-s period of data. A 20-s interval is shown in Fig. 11*C*. The actual stretch is in black, and the ISI decoding prediction is in green. ISI decoding picked out the big peaks but cannot reconstruct the structure away from the peaks. The E_{norm} for the reconstruction of the 90-s test interval was 0.90.

In an effort to improve the reconstruction, we tried the linear filter technique described in METHODS. Using the same 90 s of the stretch waveform that generated the ISI decoding relationship, we determined the best combination of a constant S_0 and kernel $K(t)$. The optimum kernel is shown in Fig. 11*B*. The corresponding best S_0 was 0.18 mm. We used *Eq. 1* to reconstruct the stimulus from the spike times during the 90-s test interval and obtained an E_{norm} of 0.73. A 20-s portion of the reconstruction is shown in red in Fig. 11*C*. The reconstruction is much better than that obtained with ISI decoding. In particular, the amplitude is predicted accurately in response to clusters of spikes. This indicates that the assumption of linearity is justified and that spike rate adaptation does not prohibit reconstruction of a waveform containing these frequencies. The

Journal of Neurophysiology

Downloaded from jn.physiology.org on November 10, 2005

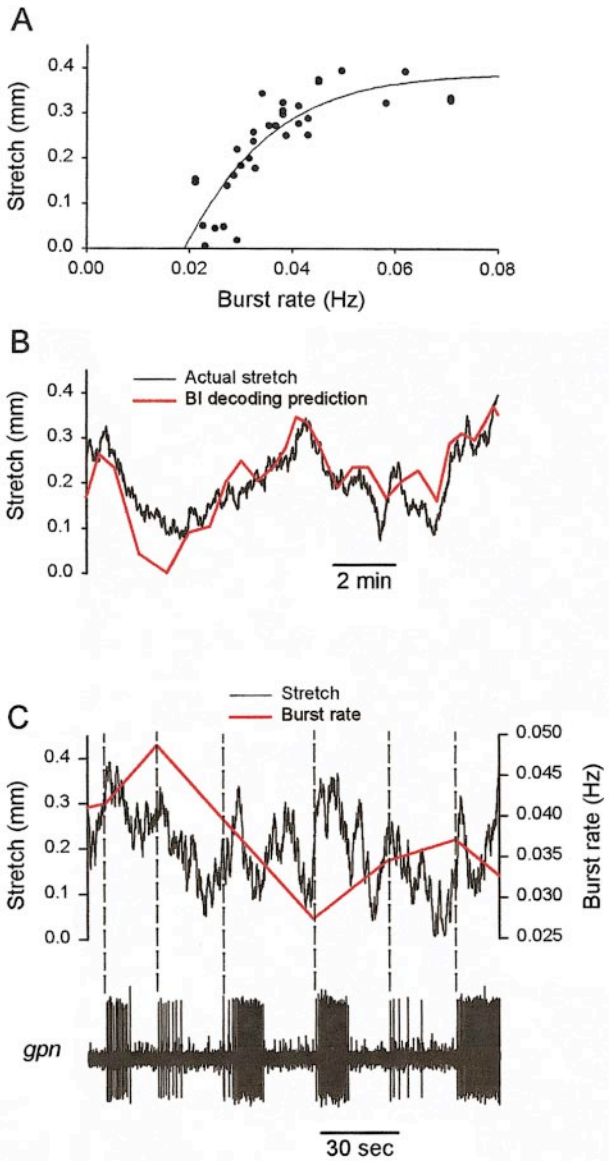

FIG. 9. Burst intervals can be used to reconstruct a slowly varying stretch waveform. A bursting mode GPR2 neuron was stretched with 30 min of white noise filtered with a time constant τ = 1,000 s. *A*: 1st 15 min were used to construct a function $\bar{S}(R)$ relating the stretch to the instantaneous bursting rate (the inverse of the burst interval). Solid circles are the experimentally measured data points, and the solid curve is a fit to the data (see text). *B*: burst interval (BI) decoding method was tested on the 2nd 15 min. Burst interval was calculated at the start time of each burst t_i, and the stretch was predicted to be $\bar{S}[R(t_i)]$. Between bursts, R(t) was obtained using linear interpolation. The actual stretch waveform is the black curve, and the prediction of BI decoding is shown in red. *C*: bursts are triggered by positive slopes in the stretch waveform during faster waveforms. *Top panel*: imposed filtered (τ = 10 s) white noise stretch (black) and calculated burst rate (red). *Bottom panel*: extracellular recording of GPR2 bursting mode response. Dashed vertical lines indicate start times of bursts.

typical period of the pyloric rhythm is 1 s, and hence a linear filter might be useful for decoding spikes generated by such a waveform.

DISCUSSION

It is difficult for a neuron to encode in its spike train a stimulus that sometimes changes extremely slowly (hours), but in other situations fluctuates from second to second. If the firing rate of the neuron is nonadapting, the neuron can report unambiguously about slowly varying stimuli. To describe a

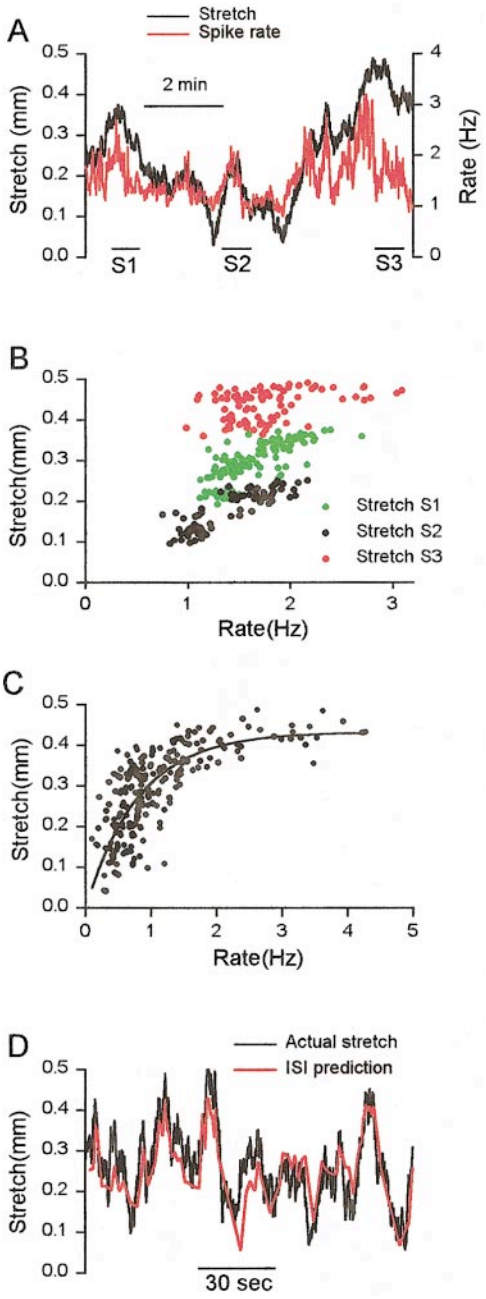

FIG. 10. Interspike intervals cannot be used to reconstruct a slowly varying waveform but can be used to reconstruct a more rapidly varying stretch waveform when the GPR2 neuron is in the spiking mode. *A*: instantaneous firing rate (red trace) of spiking mode GPR2 neuron in response to filtered (τ = 1,000 s) white noise muscle stretch (black trace). *B*: the relationship between stretch and instantaneous firing rate is plotted for the 3 40-s intervals S1, S2, and S3 shown in *A*. *C*: a spiking mode GPR2 neuron was stretched for 10 min using a white noise waveform with τ = 10 s. The 1st 5 min were used to construct a function $\bar{S}(R)$ relating the stretch to the instantaneous spiking rate, the inverse of the ISI. Solid circles are the experimentally measured data points, and the solid curve is a fit to the data (see text). *D*: the ISI decoding method was tested on the 2nd 5 min of the experiment. The ISI was calculated at each spike time t_i, and the stretch was predicted to be $\bar{S}[R(t_i)]$. A portion of the test interval is shown. The actual stretch waveform is the black trace, and the ISI decoding prediction is the red trace.

Journal of Neurophysiology

Downloaded from jn.physiology.org on November 10, 2005

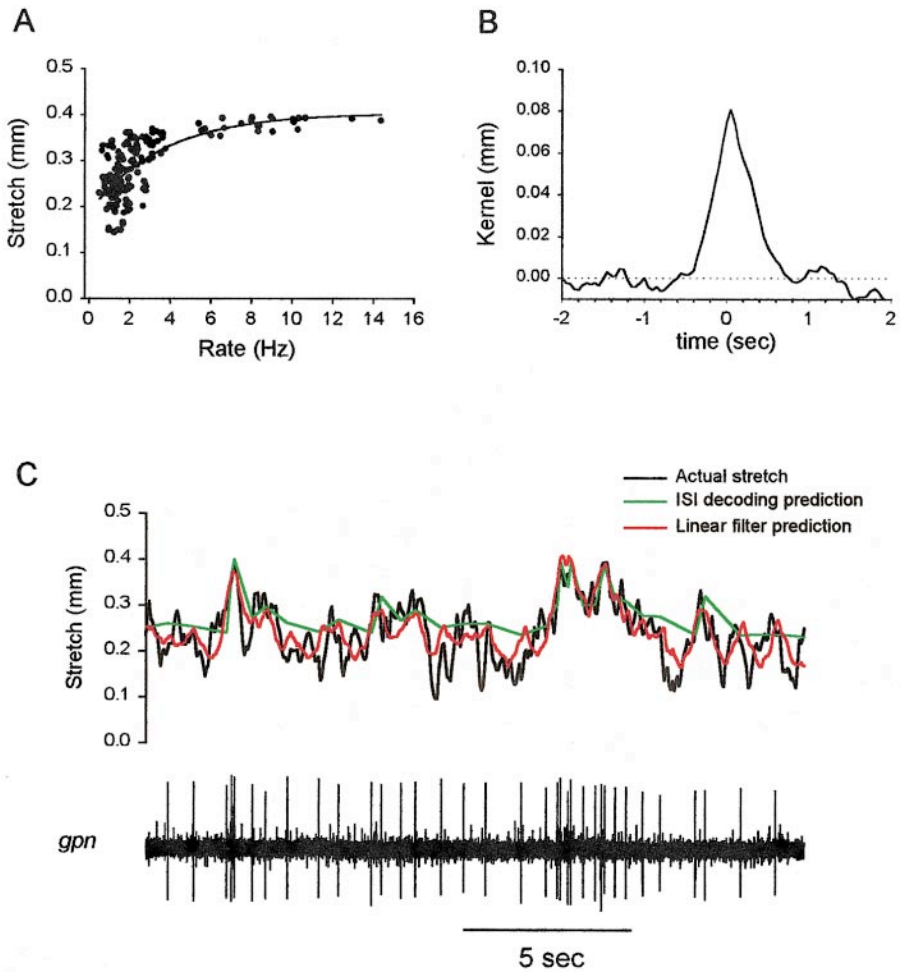

FIG. 11. A linear filter decodes spike trains when the stretch is very rapidly varying. A spiking mode GPR2 neuron was stretched for 3 min using a filtered white noise waveform with $\tau = 0.3$ s. *A*: the 1st 90 s were used to construct a function $\hat{S}(R)$ relating the stretch to the instantaneous bursting rate. Solid circles are the experimentally measured data points, and the solid curve is a fit to the data (see text). *B*: the same 90 s were also used to construct the best combination of a constant offset and linear kernel (shown). *C*: the ISI decoding method and the linear filter were tested on the spike train generated during the final 90 s of the experiment. A portion of the stimulus is shown in black. The ISI decoding prediction is shown in green. The reconstruction using the linear filter is shown in red.

rapidly varying stimulus, on the other hand, requires the ability to fire at high frequencies over short durations. This may involve firing frequencies that cannot be maintained over extended periods of time.

We have found that the GPR2 sensory neuron in the crab stomatogastric nervous system can encode accurately muscle movements that vary on times scales of both 1 s and 1,000 s. Two firing modes, spiking and bursting, are used. Faster stimuli are encoded in the spiking mode by interspike intervals. Extremely slow stimuli can be described in the bursting mode, where the stretch is encoded in the burst interval.

GPR2 bursting mode encodes sensory information about slow muscle movements

There is very little in the literature about how sensory neurons in general, and mechanoreceptors in particular, might use bursts to encode sensory information. Oscillations have been observed in a number of mechanosensory systems, including hair cells (Fuchs et al. 1988; Sugihara and Furukawa 1989) and muscle spindles (Sokabe et al. 1993), but these oscillations are at high frequencies (5–250 Hz), and their encoding significance is unclear. Another mechanoreceptor that might use bursts to encode sensory information is the anterior gastric receptor (AGR) (Combes et al. 1997; Simmers and Moulins 1988), also found in the crustacean stomatogastric nervous system. There are important differences in the ways in which GPR2 and AGR encode stretch using bursts. The increase in the GPR2 bursting rate resulting from muscle stretch does not adapt, and hence the burst interval can unambiguously describe the DC stretch amplitude. The bursting in AGR is much faster than in GPR2 with a typical frequency of 0.5–2 Hz. An AGR burst contains 5–10 spikes and lasts 100–200 ms. In response to a short (<5-s duration) stretch of *gm1*, the muscle innervated by AGR, burst frequency and spike frequency rise, whereas the burst duration decreases. However, the increases in the bursting and firing rates begin to reverse immediately after the stimulus onset and have almost completely adapted after only 4 s. An AGR burst code thus would be history dependent and only able to describe rapidly varying stretches.

Two GPR2 modes encode information about movement on two different time scales

We observed spiking and bursting modes of GPR2 activity in isolated neuromuscular preparations. Previous investigations have shown that both modes occur in minimally dissected, semi-intact preparations (Katz et al. 1989), and hence they both appear to be physiologically relevant. In the bursting mode, GPR2 reports slow DC movements but ignores faster AC movements. In the spiking mode, GPR2 fires more rapidly in response to AC movements than to DC stretches. The two GPR2 modes allow the encoding of

Journal of Neurophysiology

Downloaded from jn.physiology.org on November 10, 2005

information about muscle movements that vary on time scales of both a few seconds and many minutes. What sensory stimuli on these time scales would GPR2 likely encounter in vivo? The faster time scale most likely corresponds to rhythmic muscle movements during an ongoing motor pattern. In this mode, GPR2 appears to provide feedback to the STG on a cycle-by-cycle basis. Peripheral feedback from proprioceptors can be used to ensure precise timing of central pattern–generated movement in response to changing conditions (Pearson 1993). Katz et al. (1989) found that GPR neurons responded to muscle movements generated by the gastric mill rhythm, but not the pyloric rhythm, in semi-intact preparations. We found that ISI decoding was best able to reconstruct filtered white noise stretches with a characteristic time of 10 s. Thus an ISI decoding scheme would be well suited for gastric mill motor movements.

The GPR2 bursting mode is best able to encode stretches that vary with characteristic times of many minutes rather than stretches with time courses characteristic of the STG motor patterns. What could cause a DC-like stretch of the innervated muscles? All of the intrinsic muscles in the stomatogastric nervous system insert on ossicles attached to the stomach wall or to the wall itself. When the foregut is filled with food, these muscles are stretched. The process of the clearing of food from the foregut takes several hours (Fleischer 1981). The bursting mode thus might provide the STG with a report of the clearing of the foregut of food, unaffected by the ongoing motor program. In this mode, GPR2 would no longer participate in a cycle-by-cycle feedback loop but would simply provide long-term sensory and modulatory input to the circuit.

AGR is similar to GPR2 in that it operates in both a spiking and a bursting mode. AGR differs from GPR2 in that both AGR modes respond most vigorously to stretch stimuli with a similar characteristic time scale (~1 s) (Combes et al. 1997). Although it is possible that a careful study of the two AGR modes might reveal that different characteristics of the stretch (e.g., amplitude or velocity) can be encoded better using one of the modes, it is unlikely that the modes can effectively encode stimuli on two radically different time scales.

Muscle activity triggers the switch into the bursting mode

More than one-third of the preparations initially in the spiking mode started to burst during the stretch experiments. The transition into the bursting mode thus seems to be triggered by muscle stretch. One possibility is that the transition may result from a change in the neuromodulatory environment, triggered by muscle activity. In the AGR experiments it was observed that exogenous application of the peptide TNRNFLRF-NH_2 could rapidly and reversibly trigger a switch from the spiking to the bursting mode (Combes et al. 1997). However, in our experiments, the switch in GPR2 was obtained without the exogenous application of any neuromodulatory agent, and hence, if the bursting were the result of neuromodulation, the responsible neuromodulator must originate in the preparation itself. GPR2 uses acetylcholine, serotonin, and an allatostatin-like peptide as neurotransmitters (Katz et al. 1989; Skiebe and Schneider 1994). We think it unlikely that the bursting results from automodulation using one these transmitters, because we were not able to induce bursting in unstretched spiking preparations through bath application of high concentrations of serotonin (5-HT), allatostatin-3, or the muscarinic agonist pilocarpine. We conclude that the transition either results from the release by GPR2 of an as yet unidentified neuromodulatory substance or is due to some process internal to GPR2 that is triggered by muscle stretch.

Spiking and bursting may have different synaptic targets

The use of a spiking and a bursting mode by GPR2 may be correlated with the dynamics of its release of neurotransmitters. The synaptic connections of GPR2 in the STG and anterior ganglia are complicated. The GPR neurons make rapid, cholinergic excitatory synapses onto at least five STG motor neurons. An examination of the dynamics of these synapses suggests that spikes and bursts may be differentially effective in driving different STG neurons. The postsynaptic potentials in the lateral gastric (LG) neuron resulting from GPR action potentials show significant depression (Katz and Harris-Warrick 1989), and hence their effect would weaken during a GPR2 burst. The synapse from the GPR neurons to the dorsal gastric (DG) neuron, on the other hand, although initially weaker than that to the LG neuron, shows little short-term depression (Katz and Harris-Warrick 1989), and hence the DG neuron should respond strongly to a burst.

There is a large body of literature that argues that peptides are preferentially released by trains of multiple presynaptic action potentials (Cropper et al. 1990; Peng and Horn 1991; Peng and Zucker 1993; Vilim et al. 1996a,b; Whim and Lloyd 1989). Therefore it is possible that a single or even several GPR2 spikes might liberate only ACh, and that burstlike discharge is required to release the other transmitters. Several seconds of high-frequency (20 Hz) stimulation of GPR has been shown to increase the frequency of an ongoing pyloric motor pattern (Katz and Harris-Warrick 1990). Realistic burstlike GPR stimulation (5-Hz interspike frequency, 4-s burst duration, 16.7-s burst period) for 1.5–3 min has been shown to start gastric mill motor activity (Blitz and Nusbaum 1996). Many of the effects of GPR stimulation seen in the STG have been mimicked by bath application of 5-HT (Katz and Harris-Warrick 1989; Kiehn and Harris-Warrick 1992). These results suggest that one functional role for the bursting mode is to enhance release of the GPR2 cotransmitters.

GPR2 bursts and single spikes likely have different meanings. Careful study of the dynamics of the synapses that GPR2 makes in the STG will give us a better understanding of how the different temporal characteristics of muscle stretch encoded by GPR2 are decoded to affect motor patterns.

This work was supported by National Institutes of Health Grants NS-17813 and MH-46742, Individual National Research Service Award NS10564 to J. T. Birmingham, the Sloan Center for Theoretical Neurobiology at Brandeis University, and the W. M. Keck Foundation.

Address for reprint requests: E. Marder, MS 013, Volen Center, Brandeis University, Waltham, MA 02454-9110.

Received 16 April 1999; accepted in final form 3 August 1999.

REFERENCES

ABBOTT, L. F. Decoding neuronal firing and modeling neural networks. *Q. Rev. Biophys.* 27: 291–331, 1994.

BLITZ, D. M. AND NUSBAUM, M. P. Sensory neuron activation of modulatory projection neurons. *Soc. Neurosci. Abstr.* 22: 1375, 1996.

Journal of Neurophysiology

Downloaded from jn.physiology.org on November 10, 2005

COLEMAN, M. J., MEYRAND, P., AND NUSBAUM, M. P. A switch between two modes of synaptic transmission mediated by presynaptic inhibition. *Nature* 378: 502–505, 1995.

COMBES, D., SIMMERS, A. J., AND MOULINS, M. Conditional dendritic oscillators in a lobster mechanoreceptor neurone. *J. Physiol. (Lond.)* 499: 161–177, 1997.

CROPPER, E. C., PRICE, D., TENENBAUM, R., KUPFERMANN, I., AND WEISS, K. R. Release of peptide transmitters from a cholinergic motor neuron under physiological conditions. *Proc. Natl. Acad. Sci. USA* 87: 933–937, 1990.

FLEISCHER, A. G. The effect of eyestalk hormones on the gastric mill in the intact lobster *Panulirus interruptus*. *J. Comp. Physiol.* 141: 363–368, 1981.

FUCHS, P. A., NAGAI, T., AND EVANS, M. G. Electrical tuning in hair cells isolated from the chick cochlea. *J. Neurosci.* 8: 2460–2467, 1988.

HARRIS-WARRICK, R. M., MARDER, E., SELVERSTON, A. I., AND MOULINS, M. *Dynamic Biological Networks: The Stomatogastric Nervous System*. Cambridge, MA: MIT Press, 1992.

HOOPER, S. L., O'NEIL, M. B., WAGNER, R. J., EWER, J., GOLOWASCH, J., AND MARDER, E. The innervation of the pyloric region of the crab, *Cancer borealis*: homologous muscles in decapod species are differently innervated. *J. Comp. Physiol. [A]* 159: 227–240, 1986.

KATZ, P. S., EIGG, M. H., AND HARRIS-WARRICK, R. M. Serotonergic/cholinergic muscle receptor cells in the crab stomatogastric nervous system. I. Identification and characterization of the gastropyloric receptor cells. *J. Neurophysiol.* 62: 558–570, 1989.

KATZ, P. S. AND HARRIS-WARRICK, R. M. Serotonergic/cholinergic muscle receptor cells in the crab stomatogastric nervous system. II. Rapid nicotinic and prolonged modulatory effects on neurons in the stomatogastric ganglion. *J. Neurophysiol.* 62: 571–581, 1989.

KATZ, P. S. AND HARRIS-WARRICK, R. M. Neuromodulation of the crab pyloric central pattern generator by serotonergic/cholinergic proprioceptive afferents. *J. Neurosci.* 10: 1495–1512, 1990.

KIEHN, O. AND HARRIS-WARRICK, R. M. Serotonergic stretch receptors induce plateau properties in a crustacean motor neuron by a dual-conductance mechanism. *J. Neurophysiol.* 68: 485–495, 1992.

KILMAN, V. L. AND MARDER, E. Ultrastructure of the stomatogastric ganglion neuropil of the crab *Cancer borealis*. *J. Comp. Neurol.* 374: 362–375, 1996.

MAYNARD, D. M. AND DANDO, M. R. The structure of the stomatogastric neuromuscular system in *Callinectes sapidus*, *Homarus americanus* and *Panulirus argus* (decapoda crustacea). *Philos. Trans. R. Soc. Lond. B Biol. Sci.* 268: 161–220, 1974.

MULLONEY, B. AND SELVERSTON, A. I. Organization of the stomatogastric ganglion in the spiny lobster. I. Neurons driving the lateral teeth. *J. Comp. Physiol.* 91: 1–32, 1974a.

MULLONEY, B. AND SELVERSTON, A. I. Organization of the stomatogastric ganglion in the spiny lobster. III. Coordination of the two subsets of the gastric system. *J. Comp. Physiol.* 91: 53–78, 1974b.

PEARSON, K. G. Common principles of motor control in vertebrates and invertebrates. *Annu. Rev. Neurosci.* 16: 265–297, 1993.

PENG, Y. AND ZUCKER, R. S. Release of LHRH is linearly related to the time integral of presynaptic Ca^{2+} elevation above a threshold level in bullfrog sympathetic ganglion. *Neuron* 10: 465–473, 1993.

PENG, Y.-Y. AND HORN, J. P. Continuous repetitive stimuli are more effective than bursts for evoking LHRH release in bullfrog sympathetic ganglia. *J. Neurosci.* 11: 85–95, 1991.

RIEKE, F., WARLAND, D., DE RUYTER VAN STEVENINCK, R., AND BIALEK, W. *Spikes: Exploring the Neural Code*. Cambridge, MA: MIT Press, 1997.

SIMMERS, J. AND MOULINS, M. Nonlinear interneuronal properties underlie integrative flexibility in a lobster disynaptic sensorimotor pathway. *J. Neurophysiol.* 59: 757–777, 1988.

SKIEBE, P. AND SCHNEIDER, H. Allatostatin peptides in the crab stomatogastric nervous system: inhibition of the pyloric motor pattern and distribution of allatostatin-like immunoreactivity. *J. Exp. Biol.* 194: 195–208, 1994.

SOKABE, M., NUNOGAKI, K., NARUSE, K., SOGA, H., FUJITSUKA, N., YOSHIMURA, A., AND ITO, F. Plateau pattern of afferent discharge rate from frog muscle spindles. *J. Neurophysiol.* 70: 275–283, 1993.

SUGIHARA, I. AND FURUKAWA, T. Morphological and functional aspects of two different types of hair cells in the goldfish sacculus. *J. Neurophysiol.* 62: 1330–1343, 1989.

VILIM, F. S., CROPPER, E. C., PRICE, D. A., KUPERFERMANN, I., AND WEISS, K. R. Release of peptide cotransmitters in *Aplysia*: regulation and functional implications. *J. Neurosci.* 16: 8105–8114, 1996a.

VILIM, F. S., PRICE, D. A., LESSER, W., KUPFERMANN, I., AND WEISS, K. R. Costorage and corelease of modulatory peptide cotransmitters with partially antagonistic actions of the accessory radula closer muscle of *Aplysia californica*. *J. Neurosci.* 16: 8092–8104, 1996b.

WHIM, M. D. AND LLOYD, P. E. Frequency-dependent release of peptide cotransmitters from identified cholinergic motor neurons in *Aplysia*. *Proc. Natl. Acad. Sci. USA* 86: 9034–9038, 1989.

Journal of Neurophysiology

Downloaded from jn.physiology.org on November 10, 2005